

# Structure and phase transformations in uranium metal

J.D. Axe

Brookhaven National Laboratory, Upton, NY (USA)

G. Grübel

European Synchrotron Radiation Facility, Grenoble (France)

G.H. Lander

Institute for Transuranium Elements, Karlsruhe (Germany)

## Abstract

In common with other elemental actinides, metallic uranium exists in several allotropic forms, differing from one another by complex but subtle atomic rearrangements. This article reviews progress in understanding the successive phase transformations from the perspective of soft-mode instabilities.

## 1. Soft mode phenomena

Certain structural phase transformations in solids result from a vibrational instability in the material. These are termed “soft-mode” displacive transformations, and the associated soft-mode concept provides a unifying perspective [1, 2]. This idea, combined with simple symmetry arguments and free energy considerations, provides a useful tool by which the phase behavior of materials can be systematized and understood at the phenomenological level.

Any phase transformation can be characterized by an order parameter, *i.e.* a quantity which is non-zero in one of the phases but which vanishes in the other. Order parameters for displacive phase transformations are defined in terms of what may be called a phonon expansion, such that

$$\mu_{ik}(t) = \sum_{q,j} \xi_k(qj) Q_{qj}(t) \exp(iql) \quad (1)$$

The displacement of the  $k$ th atom in the  $l$ th unit cell is decomposed into normal modes which are plane waves with a wave vector  $q$  and a branch label  $j$ . (There are three acoustic branches and  $3N - 3$  optical branches, if there are  $N$  atoms in the unit cell.) Each mode has a polarization vector  $\xi_k(qj)$  specifying the pattern of the displacements, and an amplitude  $Q_{qj}(t)$  called the normal coordinate. Any arbitrary set of displacements can be decomposed in this way. In a soft-mode displacive transformation, the resulting average static atomic displacements resemble the frozen-in-pattern of vibrations from a single normal mode with wave vector  $q_s$ . In

other words, the order parameter can be chosen as a static component  $\langle Q_{qsj} \rangle$  of a single normal mode. The displacements are always referred to the more symmetric of the two phases, and their appearance will generally produce a less symmetric phase.

Not all structural transformations can be described by a single normal mode; in fact, most (including seemingly simple examples, such as face-centered cubic (f.c.c.) to hexagonal close-packed (h.c.p.)) cannot. When such a description is possible, the natural presumption is to implicate the phonon in question in the mechanism of the transformation. The dynamics of a phase transformation concern the time-dependent fluctuations of the order parameter, *i.e.* the phonons. At a continuous, or second-order, transformation, the amplitudes of these fluctuations diverge and, since phonon amplitudes are inversely proportional to the square of their vibrational frequency  $\omega^2(q)$ , one is led to the proposition that  $\omega^2(q_s) \rightarrow 0$  along the phase boundary.

## 2. $\alpha$ -Uranium

The simple body-centered cubic (b.c.c.) structure is the stable, highest temperature solid modification of a majority of the simple metals. B.c.c. metals tend to have lower phonon energies and, thus, higher vibrational entropy than their f.c.c. counterparts [3, 4]. The high temperature phase diagram of uranium metal is shown in Fig. 1. Not surprisingly,  $\gamma$ -U, which is the stable phase in equilibrium with the liquid, has b.c.c. structure. Therefore, it is natural to choose b.c.c. as the parent

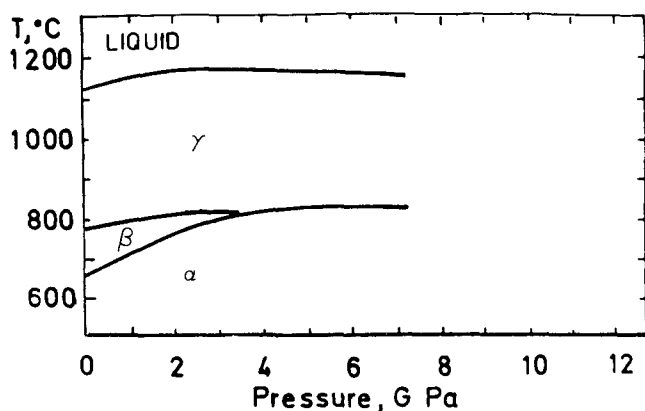


Fig. 1. High temperature phase diagram for uranium.

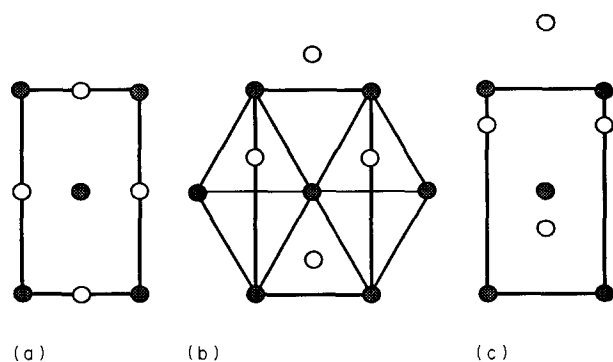


Fig. 2. Transformations induced by [110] TA displacements on a b.c.c. lattice: (a) [110] planes of the b.c.c. structure ( $Im\bar{3}m$ ), where the open circles represent atoms in the plane above those represented by shaded circles; (b) shifting alternate layers along [1-10] (and stretching the long- to short-axis ratio from  $2^{1/2}$  to  $3^{1/2}$ ) produces a h.c.p.-like structure ( $P63/mmc$ ); (c) further shifting of alternate layers produces the  $\alpha$ -U structure ( $Cmcm$ ).

structure in which to elaborate the remaining structures. (Th, Pa, Np and Pu also have stable high temperature b.c.c. phases, and this is the natural starting point for an inclusive structural “theory” of all the known actinide metals.)

The structural changes associated with the  $\gamma$ -U-to- $\beta$ -U transformation have been discussed recently [5], but are too complex to discuss here, and certainly do not represent a single-phonon mode. In contrast, the  $\gamma$ -U-to- $\alpha$ -U transformation lends itself naturally to a “soft-mode” description. Formally, the  $\alpha$ -U structure results from the freezing-in of a transverse acoustic (TA) normal vibrational mode of the b.c.c. structure with a wave vector  $q = [\frac{1}{2}, \frac{1}{2}, 0]$ , i.e. with alternate [110] planes displaced in opposing [1-10] directions, as shown in Fig. 2. The relative displacement of the adjacent planes is quite large but the pattern is precisely correct. In particular, the centered orthorhombic unit cell requires that all atoms within a given [110] plane be displaced identically. There are additional long-wavelength elastic distortions that contract the unit cell in the [001] b.c.c. direction (the  $a$  direction in  $\alpha$ -U), while

expanding the lattice along the [1-10] direction, approximately preserving the crystal volume. However, these secondary elastic distortions are required by basic symmetry arguments, so are “built-in” to a soft-mode description in a satisfactory way. On this basis, there is a strong presumption that transverse phonon anomalies exist in  $\gamma$ -U. Unfortunately, to our knowledge, corroborative neutron scattering experiments have not been attempted.

One odd thing about the  $\gamma$ -U-to- $\alpha$ -U transformation (assuming this is the correct mechanism) is that, in the process of shifting, the [110] planes pass through and reject an h.c.p. phase, which occurs for a relative displacement of  $2^{1/2}a/6 = 0.83 \text{ \AA}$ , i.e. about half that required for  $\alpha$ -U, as shown in Fig. 2. Presumably, the fact that most materials do not pass up an opportunity to form a close-packed arrangement accounts for the unpopularity of the  $\alpha$ -U structure in other regions of the periodic table, although it does occur for other actinides (Am-IV, Cm-III, Bk-III and Cf-III). This is made additionally plausible by the remarkable fact that the h.c.p. structure is not found among the actinides. The “double h.c.p.” structure (Am-I, Cm-I, Bk-I and Cf-I) derives from a freezing-in of a different TA phonon with wave vector  $[\frac{1}{4}, \frac{1}{4}, 0]$  [5].

### 3. The puzzle of low temperature $\alpha$ -Uranium

The  $\alpha$ -U structure is as close as uranium comes to realizing a close-packed structure, and Fig. 1 reveals no additional low temperature phases. Nevertheless, by 1980, a variety of measurements, including anomalies in electron transport [6], elastic compliance [7] and thermal expansion [8], hinted at the existence of not one but three additional low temperature phase transformations at 43, 37 and 22 K. However, diffraction experiments designed to detect changes in crystal structure or the onset of magnetic order had failed [9]. It has taken another decade to sort out the puzzle.

Progress began with the measurement of the room temperature lattice dynamics, using inelastic neutron scattering techniques [10]. Figure 3 shows the phonon energies plotted against their wave vector along the principal symmetry directions for the  $\alpha$ -U structure. The deep minimum in the  $\Sigma_4$  branch at  $q = [\frac{1}{2}, 0, 0]$ , indicative of a tendency of adjacent [100] planes to dimerize, is quite unusual. Furthermore, the minimum phonon frequency shows a classical “soft-mode” behavior, moving to a lower frequency upon lowering the temperature, reaching a minimum at about 70 K, and stiffening (moving to higher frequency) somewhat thereafter. Furthermore, a low temperatures, weak elastic (Bragg) scattering was observed to persist at (or at least very near) the positions in reciprocal space where

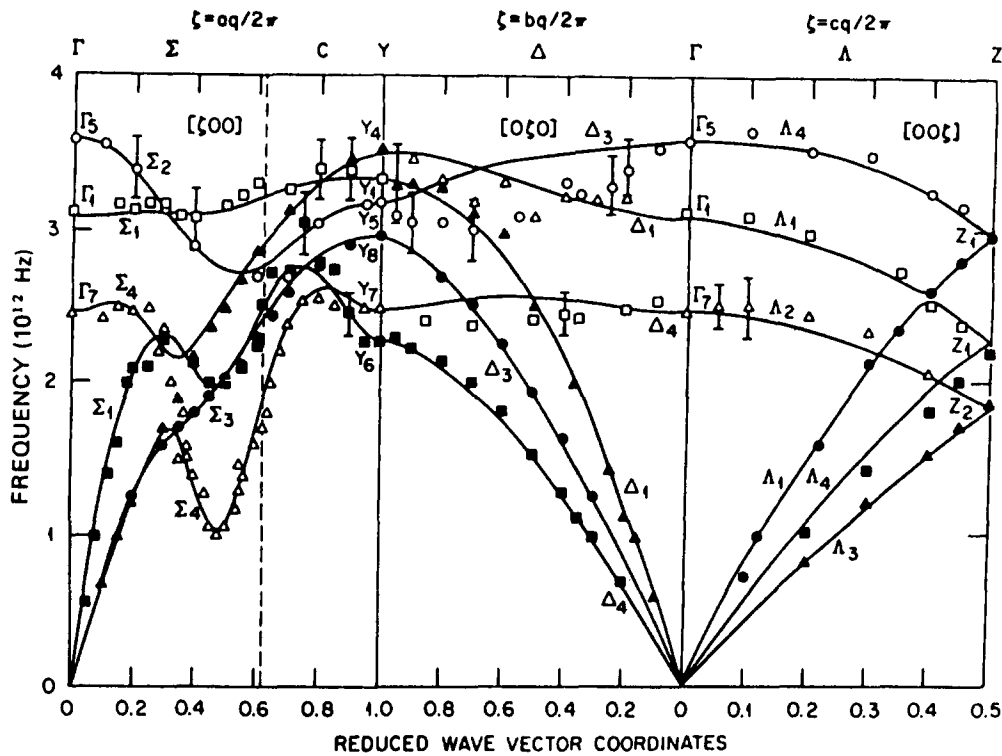


Fig. 3. Phonon energy vs. wave vector along symmetry directions in  $\alpha$ -U. Anomalous dispersion indicative of soft-mode behavior is seen in the TA branch labelled  $\Sigma_4$  (after ref. 11).

the inelastic scattering occurred [11]. While the peaks, known as the "Smith peaks", were the first solid diffraction manifestations of the structural modifications taking place, they only raised two further difficulties:

- (1) they occurred at an onset temperature (about 60 K) considerably higher than those suggested by the anomalies in the bulk properties discussed above;
- (2) more fundamentally, they made no "sense" as modulations of the  $\alpha$ -U structure.

This second point requires further discussion. Conventional soft-mode phonon condensation modulates the parent structure in such a way as to leave the parent Bragg peak positions unaffected but causes each of them to be decorated with new Bragg "satellites". The Smith peaks could be classified according to this scheme, but only as satellites of unobserved "ghost" parent Bragg peaks with a lattice constant differing by about one part in  $10^3$  from the one actually observed. The discrepancy was small but impossible to dismiss. The understanding of this "ghost" lattice was the last piece of the puzzle to fall into place.

#### 4. Incommensurate modulation

In the course of attempting to sort out the Smith peaks, a new set of diffraction satellites was discovered [12], which further detailed investigations [13] showed

to suffer from none of the difficulties discussed above. Although weak (about 1% of the parent  $\alpha$ -U Bragg peaks), they were still about 100 times stronger than the original Smith peaks. The onset temperature ( $T_0 = 43$  K) agreed with the highest suggested transition temperature from the bulk measurements, and the peak positions indexed properly as modulations of the established  $\alpha$ -U structure. The reason that they had been missed in earlier investigations is that the modulation wave vector is incommensurate with that of the parent structure, so that the peaks could not be detected in Bragg peak scans along directions of high symmetry.

When the wave vector  $q_s$  of the modulation cannot be related to the periodicity of the underlying lattice by multiplication by a rational number, the structure is said to be incommensurate. Other examples of incommensurate structures occur in surface reconstruction, quasi-crystals and in some antiferromagnets. In metals, incommensurate displacive transformations may result from a charge density wave (CDW) in the conduction electrons near the Fermi surface [14]. The atomic cores displace in response to the electric fields set up by the CDW. CDW instabilities are favored when two large portions of the Fermi surface differ by the wave vector  $q_s$  (Fermi surface nesting). This is most common for quasi-one- [15] or quasi-two-dimensional [16] metals, because the Fermi energy is then independent of some component(s) of the electron

momenta. The phonon mode softening in CDW transformations is brought about by conduction electron screening effects (giant Kohn anomalies) [17] but classical examples of incommensurate soft-mode transformations occur in insulators as well as in metals [18].

As discussed above, the diffraction from a modulated lattice causes each of the parent Bragg peaks  $[HKL]$  to be decorated with Bragg satellites, which appear at the positions  $(hkl) = (H \pm q_x, K \pm q_y, L \pm q_z)$ , where  $q_s = (q_x, q_y, q_z)$  is the soft-mode wave vector. The measured values for  $q_s$  at temperatures near  $T_0$  are approximately (0.49, 0.13, 0.22) and, since all the components of  $q_s$  are non-zero, there are eight satellites about each parent Bragg reflection. The nature of the modulation displacement pattern has been deduced from a study of the intensities of the satellite peaks [12]. The intensities are well reproduced by a sinusoidal displacement pattern, with the largest displacement amplitude (0.027 Å) along the [100] direction. The displacement pattern

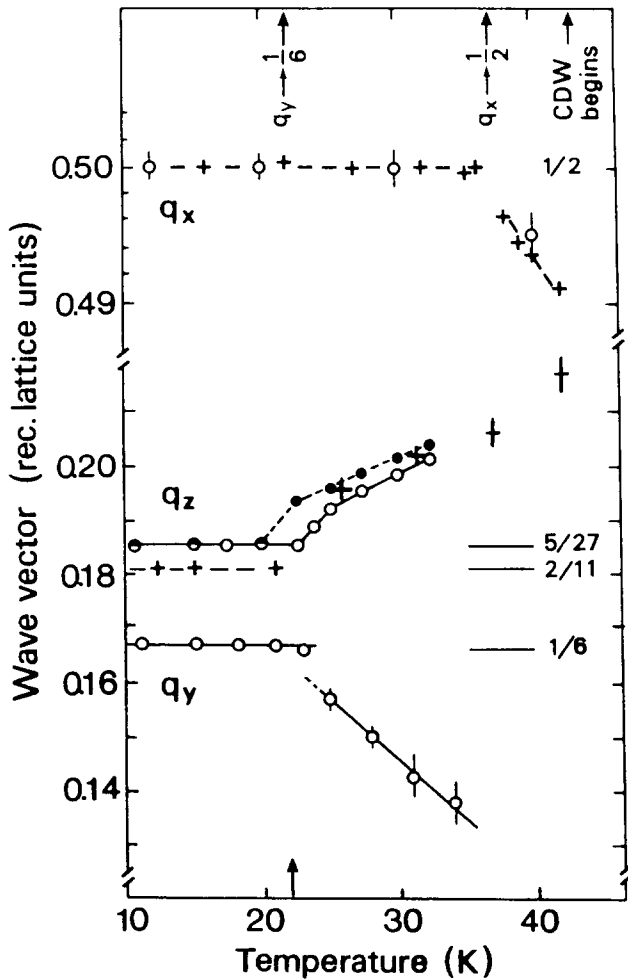


Fig. 4. Temperature dependence of the modulation wave vector in  $\alpha$ -U at low temperature, showing lock-in transformation at  $T=37$  and 22 K. Plus signs (circles) refer to X-ray (neutron) data (after ref. 19).

is consistent with that required by symmetry for a  $\Sigma_4$  phonon mode, confirming the soft-mode nature of the instability.

5. Lock-in transformations

The discovery of the incommensurate soft-mode instability resolved the nature of the transformation at 43 K but did not clarify the lower temperature anomalies at 37 and 22 K. The key to the further understanding of these effects came from careful synchrotron X-ray (and later neutron) diffraction experiments, which determined the exact wave vector  $q_s$  and its variation with temperature [19]. A summary of these results is shown in Fig. 4. Between 43 and 37 K, all the components of  $q_s$  change smoothly; however, below 37 K,  $q_x$  is frozen at  $\frac{1}{2}$ . Similarly,  $q_y$  and  $q_z$  vary freely until 22 K, where they become frozen at rational values.

The behavior of  $q_x$  observed at 37 K had been previously predicted on theoretical grounds [20]. It is an example of incommensurate lock-in – a phenomenon common in the study of incommensurate structures [16]. An incommensurate sinusoidal modulation of the form of eqn. (1) continuously goes in and out of phase with the underlying periodic lattice, and extracts no net interaction energy. (In fact, the phase of the modulation with respect to the lattice is freely variable, giving rise to a “phason” degree of freedom.) However, by adding multiple harmonics to the spatial modulation

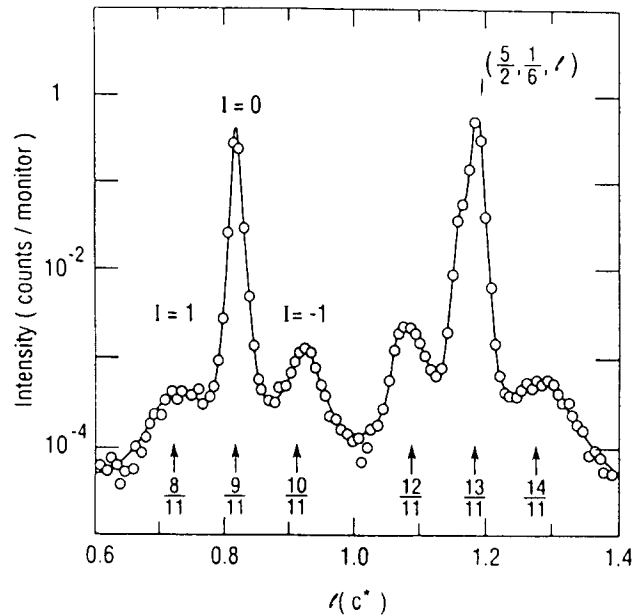


Fig. 5. X-ray diffraction scan at 22 K, showing primary modulation satellites at values of  $l = 1 \pm \frac{2}{11}$ , each surrounded by a pair of weaker secondary satellites displaced by  $\Delta l = \pm \frac{1}{11}$ . This pattern confirms the existence of phase-slip defects in the low temperature phase of  $\alpha$ -U (after ref. 19).

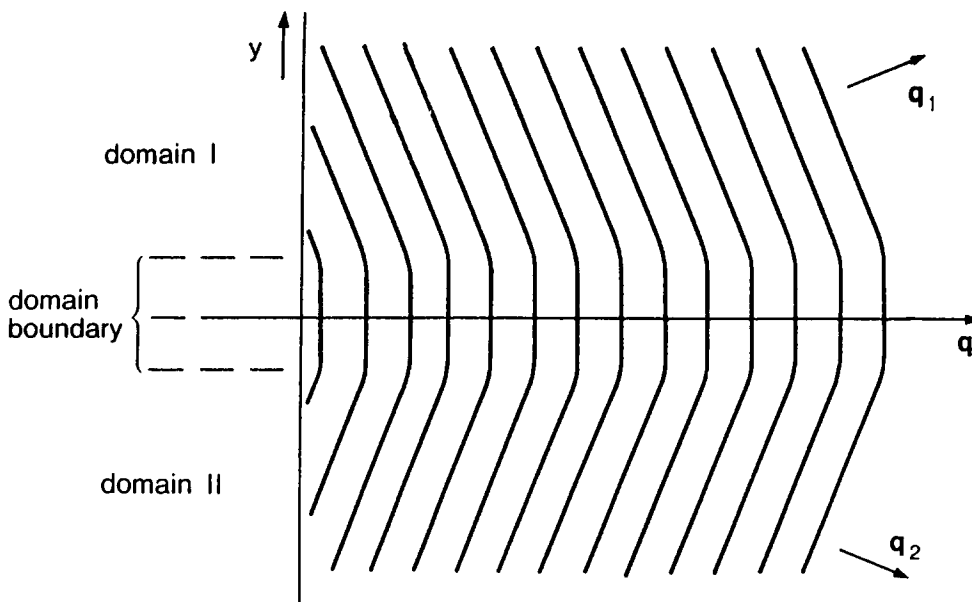


Fig. 6. Schematic representation of the domain boundary region in low temperature  $\alpha$ -U. The lines represent the nodal planes of the sinusoidal modulation. It should be noted that the wave vector is along the symmetric  $[100]$  direction within the boundary region (after ref. 22).

with appropriate phasing, the regions with favorable (unfavorable) interaction can be expanded (contracted), so gaining further overall stabilization of the modulation. Careful consideration reveals that this process also drives the fundamental wave vector  $q_s$  toward a submultiple of the periodicity of the underlying lattice [21], leading to the lock-in observed behavior.

The  $q_x$  lock-in is driven by fourth-order terms in the amplitude of the primary harmonic displacement. Grübel *et al.* [19] extended the work of Walker [20] to show how sixth-order terms in the amplitude would cause both  $q_y$  and  $q_z$  to lock-in simultaneously to the value  $\frac{1}{6}$ . Figure 4 shows that the observed value is  $q_y = \frac{1}{6}$ , whereas  $q_z$  takes a slightly different value of  $\frac{2}{11}$  or  $\frac{5}{27}$ , *i.e.* close to but not equal to  $\frac{1}{6}$ . This can be explained by introducing into the  $q_z = \frac{1}{6}$  structure occasional phase slips, where the modulation changes not by the prescribed value  $\phi = 2\pi/6$  between adjacent unit cells along the  $c$  axis but by twice that amount. If, on average, there is one phase slip for every  $n$  unit cells and they repel one another, they can form a regular array with an average wave vector  $q_z = (1 + 1/n)/6$ . Thus, the  $q_z = \frac{2}{11}$  and  $\frac{5}{27}$  structures are easily recognized as the  $n = 11$  and  $n = 9$  phase-slip defects in the basic  $q_z = \frac{1}{6}$  structure. The diffraction signature of such a phase-slip structure consists of another hierarchy of diffraction peaks that decorate the primary satellites in much the same way that the primary satellites decorate the main Bragg peaks. The correctness of the above explanation was confirmed with the observation of these phase-slip satellites as shown in Fig. 5 [19].

## 6. A ghost story

The remaining puzzle of  $\alpha$ -U is the occurrence of the anomalous Smith peaks that seem to arise from diffraction from a "ghost" lattice with a different lattice spacing. A way to understand this phenomenon has been proposed recently by Yamada [22]. In reality, there are four distinct but equivalent  $\alpha$ -U structures below 37 K, corresponding to modulation wave vectors  $q_s = (\frac{1}{2}, \pm q_y, \pm q_z)$ . They differ only in the phase relationship of the various sinusoidal components of the displacements. In general, a given specimen will be divided roughly equally into domains of each type. In the region that separates two domains, the modulation wave vector changes smoothly, as shown schematically in Fig. 6. Yamada showed by symmetry that, in the interior of each domain, there is a uniaxial strain  $e_{11}$  along the  $x$  axis, which is proportional to  $[q_y^2 + q_z^2]$ , producing an identical transformation-induced strain within all the domains. However, this strain vanishes within the domain boundary region where  $q_y = q_z = 0$ , leaving the region with a slightly different lattice spacing. Since, within the boundary region, the modulation wave vector points along the  $[100]$  direction, diffraction from the domain boundary regions can explain satisfactorily the existence of the Smith peaks.

## Acknowledgment

The work carried out at Brookhaven National Laboratory was supported by the Division of Material

Sciences, US Department of Energy, under Contract DE-AC02-76CH00016.

## References

- 1 W. Cochran, *Adv. Phys.*, **9** (1960) 387.
- 2 J.D. Axe and G. Shirane, *Phys. Today*, **26** (1973) 32.
- 3 C. Zener, *Elasticity and Anelasticity of Metals*, University of Chicago Press, Chicago, IL, 1948.
- 4 G. Grimvall and I. Ebbsjö, *Phys. Scr.*, **12** (1975) 168.
- 5 B. Mettout, V.P. Dmitriev, M. Ben Jaber and P. Toledano, *Phys. Rev.*, **B48** (1993) 6908.
- 6 T.G. Berlincourt, *Phys. Rev.*, **114** (1957) 969.
- 7 E.S. Fisher and H.J. McSkimin, *Phys. Rev.*, **124** (1961) 67.
- 8 M. Steinitz, C.E. Burleson and J.A. Marcus, *J. Appl. Phys.*, **41** (1970) 5037.
- 9 G.H. Lander and M.H. Mueller, *Acta Crystallogr.*, **29** (1970) 129.
- 10 W.P. Crummet, H.G. Smith, R.M. Nicklow and N. Wakabayashi, *Phys. Rev.*, **B**, **19** (1979) 6028.
- 11 H.G. Smith, N. Wakabayashi, W.P. Crummet, R.M. Nicklow, G.H. Lander and E.S. Fisher, *Phys. Rev. Lett.*, **44** (1980) 1612.
- 12 J.C. Marmeggi and A. Delapalme, *Physica B*, **120** (1980) 309.
- 13 J.C. Marmeggi, A. Delapalme, G.H. Lander, C. Vettier and N. Lehner, *Solid State Commun.*, **43** (1982) 577.
- 14 J.C. Marmeggi, G.H. Lander, S. van Smaalen, T. Brückel and C.M.E. Zeyen, *Phys. Rev. B*, **42** (1990) 9365.
- 15 H.G. Smith and G.H. Lander, *Phys. Rev. B*, **30** (1984) 5407.
- 16 A.W. Overhauser, *Phys. Rev.*, **167** (1968) 691.
- 17 R. Comès and G. Shirane, in J.T. DeVreese (ed.), *Highly Conducting One-Dimensional Solids*, Plenum, New York, 1979, p. 17.
- 18 D.E. Moncton, J.D. Axe and F.J. DiSalvo, *Phys. Rev. B*, **16** (1977) 801.
- 19 W. Kohn, *Phys. Rev. Lett.*, **2** (1959) 393.
- 20 M. Iizumi, J.D. Axe, G. Shirane and K. Shimaoka, *Phys. Rev. B*, **15** (1977) 4392.
- 21 G. Grübel, J.D. Axe, D. Gibbs, G.H. Lander, J.C. Marmeggi and T. Brückel, *Phys. Rev.*, **43** (1991) 8803.
- 22 M.B. Walker, *Phys. Rev. B*, **34** (1986) 6830.
- 23 W.L. McMillan, *Phys. Rev. B*, **14** (1976) 978.
- 24 Y. Yamada, *Phys. Rev. B*, **47** (1993) 5614.